Catalysis Today, 16 (1993) 417-426
Elsevier Science Publishers B.V., Amsterdam

Molecular Design of Supported Niobium Oxide Catalysts

Jih-Mirn Jehng and Israel E. Wachs

Zettlemoyer Center for Surface Studies Department of Chemical
Engineering Lehigh University Bethlehem, PA 18015, U. S. A.

ABSTRACT

The current investigation demonstrates that it is possible to molecularly design supported niobium oxide catalysts with the assistance of molecular characterization methods such as Raman spectroscopy. The formation and location of the surface niobium oxide species are controlled by the surface hydroxyl chemistry, and the surface niobium oxide species are located in the outermost layer of the catalysts as an overlayer. The catalyst composition is a critical parameter since it affects the presence of different niobium oxide species (several different surface species and crystalline phases), and the reactivity also varies somewhat with surface niobium oxide coverage. The preparation method is not a critical parameter since it does not appear to influence the structure or reactivity of the surface niobium oxide species. However, for silica supported niobium oxide catalysts the preparation method does affect the amount of niobium oxide that can be dispersed as a two-dimensional overlayer. Calcination temperature is an important parameter that controls the activation and deactivation of the supported niobium oxide catalysts, but calcination temperature is not critical if moderate temperatures, 400-500°C, are used. The specific oxide support is a critical parameter since it dramatically affects the reactivity of the surface niobium oxide species and determines if the surface niobium oxide site is active for redox or acid catalysis. Thus, the critical parameters that affect the catalytic properties of the supported niobium oxide catalysts are the specific oxide support and catalyst composition.

1. INTRODUCTION

Many recent studies have demonstrated that two-dimensional niobium oxide overlayers are formed when niobium oxide precursors are deposited on high surface area oxide supports such as alumina, titania, zirconia, and silica [1-16]. The molecular structures and reactivity of these surface niobium oxide species have been intensively investigated over the past few years. The major structural information about these surface niobium oxide phases has been derived from Raman

0920-5861/93/$6.00

spectroscopy characterization studies because of the molecular nature of this characterization method and its ability to discriminate between different niobium oxide species that may simultaneously be present in the catalyst [8-13]. Additional structural information has been provided by X-ray absorption studies (EXAFS/XANES) [3-7]. *In situ* Raman studies on SiO_2 supported niobium oxide catalyst indicate that only one dehydrated surface niobium oxide species corresponding to the highly distorted NbO_6 octahedral structure at 980 cm^{-1} is present. The highly distorted NbO_6 octahedra responsible for *In situ* Raman bands at 985-970 and 930-820 cm^{-1} are observed on the TiO_2 and ZrO_2 supports. Below half a monolayer coverage on the Al_2O_3 support, two kinds of dehydrated surface niobium oxide species possessing highly and moderately distorted NbO_6 octahedra with Nb=O Raman bands at 980 and 880 cm^{-1}, respectively, are present. Corresponding reactivity studies have demonstrated that these surface niobium oxide species possess the active sites for many catalytic reactions involving redox and acid surface chemistry [3-6,10,11,14-15]. The fundamental information currently available about these surface niobium oxide phases is beginning to allow us to molecularly design supported niobium oxide catalysts. The molecular design of supported niobium oxide catalysts requires that we specify the synthesis method, oxide support, catalyst composition, calcination temperature, location and structure of the surface niobium oxide species, as well as its reactivity.

2. EXPERIMENTAL SECTION

The oxide supports employed in the present study were: TiO_2 (Degussa, ~55 m^2/g), Al_2O_3 (Harshaw, ~180 m^2/g), SiO_2 (Cabot, ~300 m^2/g), and ZrO_2 (Degussa, ~39 m^2/g). The supported niobium oxide catalysts were prepared by using the aqueous impregnation method (niobium oxalate), the nonaqueous impregnation method (niobium ethoxide), and the reaction between the $Nb(\eta^3-C_3H_5)_4$ complex and the hydroxyl groups of the oxide support to form a surface niobium oxide overlayer.

The molecular structures of the supported niobium oxide catalysts were characterized by laser Raman spectroscopy under *in situ* conditions. The laser Raman spectroscope consists of a Spectra Physics Ar^+ laser producing 10-100 mW of power measured at the sample. The scattered radiation was focussed into a Spex Triplemate spectrometer coupled to a Princeton Applied Research OMA III optical multichannel analyzer. Prior to the Raman analysis, the Nb_2O_5/TiO_2 and Nb_2O_5/ZrO_2 samples were calcined at 450°C for 1 hr, the Nb_2O_5/Al_2O_3 sample was calcined at 500°C for 12 hrs, and the Nb_2O_5/SiO_2 samples were calcined at 700°C for 1hr under flowing dry air in order to diminish the fluorescent background. A 50-100 mg sample disc was held by a stationary U-shaped slot in the quartz cell. The sample was further heated by a cylindrical heating coil surrounding the quartz cell at 400°C for 30 min. Oxygen gas (Linde, 99.99%

purity) was introduced into the cell from a manifold at a rate of 50-500 cm^3/min upon dehydration. The *in situ* Raman spectra were recorded after the quartz cell was cooled down to room temperature.

The supported niobium oxide catalysts were examined for their reactivity in the methanol oxidation reaction. The reactor was operated at a constant temperature of 230°C and in the differential mode by keeping methanol conversions below 8 %. A methanol/oxygen/helium mixture of ~6/13/81 at 1 atm pressure was used as the reactant gas for all the data presented. The analysis was performed on an online gas chromatograph (GC) (HP 5840A) containing two columns (Poropak R and Carbosieve SII) and two detectors (FID and TCD). The surface acidity of the supported niobium oxide catalysts were measured with an Analect FX-6160 FTIR spectrometer by pyridine adsorption.

3. RESULTS AND DISCUSSION

It is well known that supported niobium oxide catalysts possess two-dimensional surface niobium oxide phases that are formed by the reaction of the deposited niobium oxide with the surface hydroxyls of the high surface area oxide supports. Direct evidence for the titration of the surface hydroxyls (OH) by the deposited metal oxides is obtained from *in situ* infrared studies which reveal the sequential disappearance of the support OH bands during this process [16]. The consumption of surface hydroxyls can also be monitored by CO_2 chemisorption studies since CO_2 titrates the basic surface hydroxyls [16]. Both measurements, infrared spectroscopy of surface hydroxyls and chemisorption of CO_2 on the surface hydroxyls, provide a quantitative measure of the surface coverage of the niobium oxide overlayer. Consequently, a necessary condition for the formation of surface metal oxide overlayers is the presence of reactive surface hydroxyls on the oxide support. Oxide supports such as Al_2O_3, TiO_2, and ZrO_2 have a high surface density of reactive surface hydroxyls and tend to form a close-packed monolayer of the surface niobium oxide phase, whereas, oxide supports such as SiO_2 which have a lower density of reactive surface hydroxyls do not form a close-packed monolayer of the surface niobium oxide phase (see Table 1). Recent studies employing a non-aqueous allyl preparation [5,17] have demonstrated that somewhat higher surface densities on SiO_2 can be achieved with this preparation, but still resulted in only a fraction of a close-packed monolayer. Thus, the surface hydroxyl chemistry controls the formation and location of the surface niobium oxide species present in supported niobium oxide catalysts.

The molecular structures of the surface niobium oxide species present in the niobium oxide overlayer are not well understood and the influence of surface coverage (catalyst composition), specific oxide support, preparation method, and calcination temperature need to be established. The Raman spectra of alumina supported niobium oxide catalysts reveal the presence of several different niobium oxide species on the Al_2O_3 support under *in situ* conditions [12]. For loadings less than 5 wt.% Nb_2O_5/Al_2O_3, only Raman bands at ~980 (strong) and ~883 (weak) cm^{-1} are present and their intensity increases with Nb_2O_5 loading. For loadings between 8-19 wt.% Nb_2O_5/Al_2O_3, additional *in situ* Raman bands at ~935-950 and ~630-650 cm^{-1} are also present. These Raman bands have been assigned to distorted NbO_6 octahedral groups where the higher wavenumbers correspond to the more highly distorted structures [12]. Above 19 wt.% Nb_2O_5/Al_2O_3, crystalline Nb_2O_5 phases are also present which indicates that the close-packed surface niobium oxide monolayer has been formed and all the reactive surface hydroxyls consumed [8]. Thus, the catalyst composition is a critical parameter since it influences the formation of different niobium oxide structures (especially the two-dimensional surface niobium oxide species versus the three-dimensional Nb_2O_5 crystallites).

Table 1
Monolayer loading and surface density of supported niobium oxide catalysts as a function of oxide support

Oxide support	Surface area (m^2/g)	Monolayer loading (wt.%) Nb_2O_5	Surface density ($\mu mole/m^2$) Nb_2O_5
Al_2O_3	180	19	8.0
TiO_2	55	7	9.6
ZrO_2	39	5	9.6
SiO_2	300	2	0.5

The surface acidity of the alumina supported niobium oxide catalysts were probed by pyridine infrared spectroscopy studies [14]. The addition of surface niobium oxide to alumina was initially found to increase the number, as well as acid strength, of the surface Lewis acid sites on alumina. Above 5 wt.% Nb_2O_5/Al_2O_3 loadings, the number of surface Lewis acid sites decreased and surface Brønsted acid sites were formed. It is tempting to correlate these surface acidity changes with the structural changes observed in the surface niobium oxide phases by Raman spectroscopy. However, recent studies with a series of different metal oxides supported on alumina revealed that these acidity changes are not related to structural changes in the surface metal oxide overlayer, but are simply dictated by the surface coverage of the metal oxide overlayer [16]. Thus, only surface Lewis acid sites are present below

~1/3 monolayer coverage, and at high surface coverages both surface Brønsted and Lewis acid sites are present (with the number of Brønsted sites increasing with coverage).

The reactivity of the alumina supported niobium oxide catalysts was probed by the methanol oxidation reaction. The methanol oxidation reaction is very sensitive to the nature of surface sites present in oxide catalysts. Surface redox sites (sites that are capable of being reduced and oxidized) form primarily formaldehyde as well as methyl formate and dimethoxy methane as the reaction products. Surface acid sites, Lewis as well as Brønsted, result in the formation of dimethyl ether. Surface basic sites yield CO/CO_2 as the reaction products. The oxidation of methanol over the alumina supported niobium oxide catalysts yielded dimethyl ether exclusively as the reaction product. The alumina support in the absence of surface niobium oxide also yielded dimethyl ether, but at a much lower rate. The reactivity is presented in Table 2 as a function of the niobium oxide loading. The reactivity increases with initial surface niobium oxide coverage, and further increases somewhat with increasing surface coverages. The increases at higher loadings may be due to the introduction of surface Brønsted acid sites at high surface niobium oxide oxide coverages on alumina. Thus, the reactivity of surface niobium oxide species has a slight dependence on surface coverage.

Table 2
The reactivity of Nb_2O_5/Al_2O_3 catalysts as a function of loading

wt.% Nb_2O_5/Al_2O_3	mmole/g/hr
0	64
1	323
5	240
8	320
12	600

Some research groups claim that the synthesis method is critical for forming niobium oxide monolayers that possess specific structures and reactivities. To investigate this issue, a series of Nb_2O_5/SiO_2 catalysts were synthesized by different methods: niobium oxalate in water, niobium ethoxide in propanol, and nonaqueous Nb-allyl preparation. The *in situ* Raman spectra of all these catalysts exhibit a sharp band at 975-980 cm^{-1} characteristic of the isolated surface niobium oxide species (see Figure 1). The weak and broad Raman band at ~800 cm^{-1} is due to the SiO_2 support. The Nb_2O_5/SiO_2 catalysts calcined at 700°C contain no surface compounds or bulk Nb_2O_5, and exhibit the same Raman features as those calcined at 500°C. The only difference for the higher calcination temperature was the reduced background fluorescence from the sample. Thus, the synthesis method does not appear to affect the final structure of the surface niobium oxide species on silica. However, the synthesis method does determine the maximum amount of niobium oxide present in the surface metal oxide overlayer on SiO_2 since the surface density of Nb_2O_5/SiO_2 could be increased approximately five-fold with the allyl preparation. In addition, on oxide supports with a high concentration of reactive hydroxyls the preparation method will not even affect the amount of surface niobium oxide species in the overlayer (e.g. Al_2O_3, TiO_2, ZrO_2) [11].

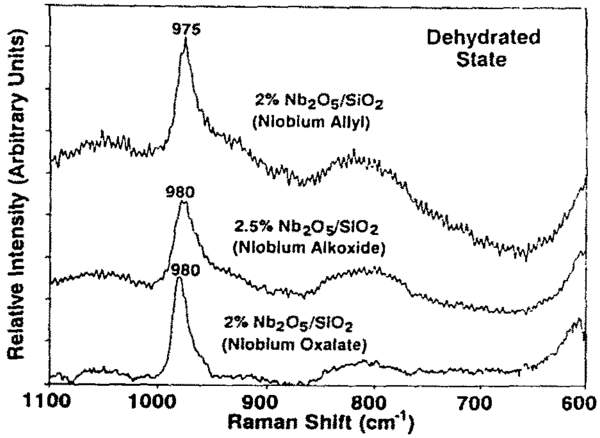

Figure 1: *In situ* Raman spectra of supported niobium oxide catalysts on silica with different preparation methods.

The nature of the supported niobium oxide phase is influenced by the calcination temperature. Moderate calcination temperatures, 350-500 °C, are required to decompose the niobium oxide precursors (oxalates, ethoxides, allyls, etc.) to form the surface niobium oxide species. Insufficient calcination temperatures do not completely decompose the precursors and, consequently, do not react with the surface hydroxyls to form the surface niobium oxide species. However, high calcination temperatures, greater than 600 °C, can result in shrinking of the surface area of the oxide support and decrease the available surface area for the surface niobium oxide species. Consequently, high calcination temperatures increase the surface coverage of the niobium oxide species and, in severe cases, destroy the surface niobium oxide phase and form crystalline Nb_2O_5 as well as compounds with the oxide supports (e.g. $AlNbO_4$) [9,11]. Thus, calcination temperature is an important parameter that controls the activation and deactivation of supported niobium oxide catalysts. However, supported niobium oxide catalysts are typically prepared by calcining at 400-500 °C which would eliminate problems with activation and deactivation.

A series of ~1 wt.% Nb_2O_5 catalysts were prepared in order to investigate the influence of different oxide supports upon the molecular structure and reactivity of the surface niobium oxide species. The low loading catalysts were selected because at these surface coverages only the isolated surface niobium oxide species is predominantly present on the different oxide supports and potential complications due to additional surface niobium oxide species could be minimized. The *in situ* Raman band due to the Nb=O bond was found to essentially be independent of the different oxide supports (see Table 3). The slight difference in band position of Nb_2O_5/ZrO_2 is due to the presence of surface Cl and F impurities on the ZrO_2 support and this band shifts to 980 cm^{-1} with increasing surface coverage of niobium oxide [12]. The important point is that the Raman spectra reveal that the same surface niobium oxide species are present on all the different oxide supports at low surface coverages. Thus, the *in situ* surface niobium oxide molecular structures are independent of the specific oxide support for low niobium oxide loadings.

The surface acidity of the supported niobium oxide catalysts were probed by pyridine adsorption using *in situ* infrared spectroscopy [14]. The Al_2O_3, TiO_2, and ZrO_2 oxide supports surfaces were only found to possess Lewis acid sites (Brønsted acid sites were not present), and the SiO_2 support surface did not possess any acid sites. Addition of low loadings of niobium oxide to the TiO_2 and ZrO_2 supports slightly decreases the number of Lewis acid sites and also decreases the strength of these acid sites. Addition of low loadings of niobium oxide to the Al_2O_3 and SiO_2 supports increases the number of Lewis acid sites, and increases the strength of the acid sites on alumina. Brønsted acid surface sites were only found for the surface niobium oxide species on alumina at high coverages [14].

Table 3
In situ Raman band position for Nb=O terminal stretching vibration as a function of oxide support for 1 wt.% Nb_2O_5 supported catalysts

Oxide Support	Raman Band for Nb=O terminal bond (cm^{-1})
SiO_2	980
TiO_2	983
ZrO_2	956
Al_2O_3	980

The reactivity of the surface niobium oxide species on the different oxide supports for 1 wt.% Nb_2O_5 was probed by the methanol oxidation reaction. The specific oxide support was found to dramatically influence the reactivity as well as selectivity of the surface niobium oxide species (see Tables 4 and 5). The surface niobium oxide species on TiO_2 and ZrO_2 were essentially inactive, but for ZrO_2 increased the selectivity towards acid products. However, the surface niobium oxide species on Al_2O_3 were extremely active for the conversion of methanol to acid products. The turnover number (TON), methanol molecules converted per Nb site per second, is approximately 10^{2-3} greater on alumina than on TiO_2 and ZrO_2. These catalytic results are in agreement with the above pyridine IR results that showed the formation of stronger Lewis acid sites on alumina, and weaker Lewis acid sites on TiO_2 and ZrO_2. In contrast, the surface niobium oxide species on SiO_2 do not yield acid products, but are active and selective for redox products. Thus, the specific oxide support is a critical parameter since it has such a profound effect on the reactivity and selectivity of the surface niobium oxide species.

Table 4
The reactivity of the methanol oxidation reaction over supported niobium oxide catalysts

	Initial Rate (mmole/g/h)			
	Al_2O_3	TiO_2	ZrO_2	SiO_2
Oxide supports	64	2.1	7.3	0.7
1 wt.% Nb_2O_5/supports	323	2.5	7.1	26.5

Table 5
The selectivity of the methanol oxidation reaction over supported niobium oxide catalysts

	Al_2O_3		TiO_2		ZrO_2		SiO_2	
	redox	acid	redox	acid	redox	acid	redox	acid
Oxide supports	0	100	9.5	90.5	58.4	5.2	-	-
1 wt.% Nb_2O_5 /supports	0	100	10.5	89.5	31.2	50.7	86.6	7.3

The origin of this dramatic support effect is due to differences in the bridging Nb-O-support bond since essentially identical terminal Nb=O bonds exist for the surface niobium oxide species on the different supports. Consequently, the oxide support cations exert a ligand effect, and not a structural effect, on the surface niobium oxide species since the oxide support controls the reactivity and selectivity of the surface niobium oxide species. A similar relationships was found for surface vanadium oxide species on different oxide supports where the reducibility of the V-O-support bond was found to control the redox reactivity [18]. The oxide supports that facilitated the reduction of the V-O-support bond (e.g. TiO_2 and ZrO_2) were found to be significantly more active than the oxide supports that retarded the reduction of the V-O-support bond (e.g. Al_2O_3 and SiO_2). It appears that an inverse of this relationship exists for the surface niobium oxide acid sites: the most active acid sites are found on the least reducible oxide support (Al_2O_3) and the least active acid sites are found on the most reducible oxide supports (TiO_2 and ZrO_2). This suggests that those surface acid sites which are most resistant to reduction will be more active during catalytic reactions. The origin of the redox behavior of the surface niobium oxide species on SiO_2 is not presently understood, but similar redox behavior has been observed for other surface metal oxides on SiO_2 [19,20]. Thus, the reactivity and selectivity of the same surface niobium oxide species (possessing the same molecular structure) is controlled by the oxide support cations which act as very powerful ligands.

4. CONCLUSIONS

The above discussion demonstrates that it is possible to molecularly design supported niobium oxide catalysts with the assistance of molecular characterization methods such as Raman spectroscopy. The formation and location of the surface niobium oxide species are controlled by the surface hydroxyl chemistry, and the surface niobium oxide species are located in the outermost layer of the catalysts as an overlayer. The catalyst composition is a critical parameter since it affects the presence of different niobium oxide species (several different surface species and crystalline phases), and the reactivity also varies somewhat with surface niobium oxide coverage. The preparation method is not a critical parameter since it does not appear to influence the structure or reactivity of the surface niobium oxide species. Calcination temperature is an important parameter that controls activation and deactivation of supported niobium oxide catalysts, but calcination temperature is not critical if moderate temperatures, 400-500 °C, are used. The specific oxide support is a critical parameter since it dramatically affects the reactivity and selectivity (redox vs. acid) of the surface niobium oxide species. In summary, the critical parameters that affect the catalytic properties are the specific oxide support and catalyst composition (or surface niobium oxide coverage).

ACKNOWLEDGMENT

The authors would to thank J. Ekerdt and R. D. Roark for preparing the niobium allyl/silica sample.

REFERENCES

1. I. E. Wachs, Proc. Intern. Conf. on Niobium and Tantalum, (1989) 679.
2. J. M. Jehng and I. E. Wachs, High Temp. Mater. and Proc., (in press).
3. M. Nishimura, K. Asakura, and Y. Iwasawa, J. Chem. Soc., Chem. Comm., (1986) 1660.
4. M. Nishimura, K. Asakura, and Y. Iwasawa, Proc. 9th Intern. Congr. Catal., 4 (1988) 1842.
5. M. Shirai, N. Ichikuni, A. Asakura, and Y. Iwasawa, Catal. Today, 8 (1990) 57.
6. S. Yoshida, Y. Nishimura, T. Tanaka, H. Kanai, and T. Funabiki, Catal. Today, 8 (1990) 67.
7. S. Yoshida, T. Tanaka, T. Hanada, T. Hiraiwa, H. Kanai, and T. Funabiki, Catal. Lett., 12 (1992) 277.
8. J. M. Jehng and I. E. Wachs, Prepn.-Am. Chem. Soc., Div. Petro. Chem., 34(3) (1989) 546.
9. I. E. Wachs, J. M. Jehng, and F. D. Hardcastle, Solid State Ionics, 32/33 (1989) 904.
10. J. M. Jehng and I. E. Wachs, Catal. Today, 8 (1990) 37.
11. J. M. Jehng and I. E. Wachs, J. Mol. Catal., 67 (1991) 369.
12. J. M. Jehng and I. E. Wachs, J. Phys. Chem., 95 (1991) 7373.
13. M. A. Vuurman and I. E. Wachs, J. Phys. Chem., 96 (1992) 5008.
14. J. Datka, A. M. Turek, J. M. Jehng, and I. E. Wachs, J. Catal., 135 (1992) 186.
15. L. L. Murrell, D. C. Grenoble, C. J. Kim, and N. C. Dispenziere, J. Catal., 107 (1987) 463.
16. A. M. Turek, I. E. Wachs, and E. DeCanio, J. Phys. Chem., 96 (1992) 5000.
17. R. D. Roark, J. Ekerdt, D. S. Kim, and I. E. Wachs, Catal. Lett., (in press).
18. G. Deo and I. E. Wachs, J. Catal., 129 (1991) 307.
19. J. M. Jehng and I. E. Wachs, Catal. Lett., 13 (1992) 9.
20. D. S. Kim and I. E. Wachs, J. Catal., 136 (1992) 209.